FULL PAPER

An Electrode Design Rule for Organic Photovoltaics Elucidated Using Molecular Nanolayers

Robert M. Cook, Lara-Jane Pegg, Sophie L. Kinnear, Oliver S. Hutter, Richard J. H. Morris, and Ross A. Hatton*

Silane nanolayers deposited from the vapor phase onto indium-tin oxide (ITO) coated glass are shown to be an effective means of tuning the work function and stabilizing the surface of this complex ternary oxide. Using this approach a pair of model hole-extracting electrodes have been developed to investigate how the performance of bi-layer organic photovoltaics is impacted by built-in positive space charge in the critical region close to the hole-extracting electrode. The magnitude and spatial distribution of positive space charge resulting from ground-state electron transfer from the donor layer to the ITO electrode upon contact formation, is derived from direct measurements of the interfacial energetics using the Kelvin probe technique. This judiciously designed experiment shows that it is unnecessary to engineer the work function of the hole-extracting electrode to match the ionization potential of the donor layer, rather only to ensure that the former exceeds the latter, thus simplifying an important aspect of device design. In addition, it is shown that silane nanolayers at the ITO electrode surface are remarkably effective at retarding device degradation under continuous illumination.

1. Introduction

Organic photovoltaics (OPV) have strong potential as a low-cost route to harvesting electricity directly from sunlight, particularly for portable consumer electronics applications and for the provision of off-grid electricity.[1–7] To realize this potential scalable and versatile strategies for optimization of the organic semiconductor/ electrode interfaces in these devices must be developed and generic design criterion identified.[7,8] The power conversion efficiency (η) of PV devices is directly proportional to the product of the short-circuit current density (J_{sc}), the voltage at the open-circuit condition (V_{oc}) and the fill-factor (FF), where the latter is defined as the ratio between the maximum-power-point and $J_{sc}.V_{oc}$. Whilst many of the factors that

control these parameters in OPVs are now well understood, current understanding of their correlation with the energetics and detailed nanostructure at organic semiconductor (polymer and small molecule)/ electrode interfaces is at an early stage of development.[5,7–11] To a large extent this is due to the intrinsic complexity of these contacts which, in the case of the most widely used substrate electrode; indium-tin oxide (ITO) coated glass, is exacerbated by the ill-defined nature and instability of the electrode itself.[12–14] It is also now clear from the large body of high quality reports in the literature pertaining to measurements of the interfacial energetics at different organic semiconductor/electrode interfaces, that the conditions under which these interfaces are formed plays a critical role in determining the interfacial energetics.[15–18] Consequently, measurements of interfacial energy level alignment are not quantitatively useful to inform device design unless the deposition and substrate conditions are exactly reproduced when fabricating devices.

This paper addresses a fundamental question relating to the design of the hole-extracting electrode in bi-layer OPV devices: When the work function (φ) of the hole-extracting electrode is greater than the ionization potential (I_p) of the donor material, how does the extent of spontaneous ground-state charge transfer from the donor layer to the hole-extracting electrode impact device performance? The answer to this question is important at a fundamental level because it advances current understanding of how charge carrier injection and transport are influenced by the interfacial energetics at this class of interface. From an applications perspective it is important because it can be used as the basis for an electrode design rule with applicability to both discrete heterojunction OPVs and device structures based on a mixed photoactive layer sandwiched between two single component layers. It is not possible to predict the impact of built-in space charge near to the electrodes on the performance of OPV devices using established models developed for doped inorganic semiconductor/electrode interfaces, owing to the limited applicability of these models to undoped organic semiconductor/electrode junctions.[15–18] To date convincing experimental evidence addressing this question has been lacking due to the difficulty in achieving large differences in the φ

R. M. Cook, L.-J. Pegg, S. L. Kinnear, O. S. Hutter,
Dr. R. J. H. Morris, Dr. R. A. Hatton
Department of Chemistry
University of Warwick
Coventry, CV47AL, United Kingdom
E-mail: ross.hatton@warwick.ac.uk
Dr. R. J. H. Morris
Department of Physics
University of Warwick
Coventry, CV47AL, United Kingdom

www.MaterialsViews.com

www.advenergymat.de

ADVANCED
ENERGY
MATERIALS

FULL PAPER

of the hole-extracting electrode without drastically modifying other properties known to be critical determinants of the energetics and nano-morphology at these interfaces. There are also surprisingly few reports correlating measurements of the energetics at organic semiconductor/ electrode interfaces directly with OPV performance[19,20] and so understanding the relationship between the detailed electronic structure at the electrode interfaces and the performance of these devices remains a fertile area of research now recognized as being critical to the development of OPVs.

The simplest organic semiconductor/electrode contact in an OPV is at the substrate electrode since the organic overlayer is typically physisorbed to the electrode surface, thereby retaining the orbital structure and chemical integrity of those molecules at the interface. The substrate electrode is also amenable to tuning of its surface potential *via* the chemisorption of a nanolayer (≤1 nm) of organic molecules that are preferentially orientated with respect to the substrate surface and have a permanent molecular dipole.[10,11,15,21–25] The power of this approach is that it decouples the bulk properties of the electrode, such as conductivity and transparency, from its surface properties such as φ and hydropilicity. As a result it has been extensively exploited as a tool to investigate the effect of modifying the Schottky barrier to charge carrier injection from the ITO electrode in the context of organic light-emitting diode research ever since the pioneering work of Willis *et al.*[22,23] and Zuppiroli *et al.*[24]. Hitherto there have been only a small number of reports pertaining to their utility in OPVs to investigate the reverse process of charge carrier extraction and in all cases OPV performance was correlated with the φ of the electrode prior to contact formation.[11,26,27] As pointed out by Kippelen[4], this approach is too simplistic to draw firm conclusions as to the relationship between the efficiency of charge carrier extraction and the interfacial energetics, since upon deposition of an organic semiconductor onto a substrate electrode there are invariably interfacial charge density redistributions and/or changes to the structure of the organic semiconductor layer that are extremely sensitive to the nature of the substrate.[15–18,26] In the context of small molecule OPV, Khodabakhsh *et al.*[11] used nanolayers of acid chloride, sulfonyl chloride and dichlorophosphate molecules deposited from solution, in conjunction with oxygen plasma treatment to tune the φ of the ITO electrode over the range 4.5–5.1 eV. The performance of bilayer OPV devices based on ITO/ copper phthalocyanine/C_{60}/bathocuproine (BCP)/Al was found to improve as a result of a large increase in J_{sc}. This improvement was attributed to better alignment between the electrode Fermi level (ε_F) and the highest occupied molecular orbital (HOMO) of the CuPc (I_p = 5.1–5.2 eV) donor layer, although the interfacial energetics were not actually measured to verify this hypothesis. Notably, the surface treatment that bought about the most significant change in device performance also dramatically increased the size of the CuPc crystallites in the critical region close to the interface with the ITO electrode. As a result, it is not possible to isolate the affect on device performance of the change in electrode φ from the impact that the change in crystallite size has on the efficiency of charge carrier transport across the CuPc/ electrode interface. Notably, the φ of the ITO electrode was also smaller than the I_p of the donor layer and so spontaneous ground-state charge transfer from the HOMO

of CuPc to the substrate electrode was not a consideration in that study. Conversely Sharma *et al.*[27] have reported that all device parameters in ITO/pentacene/C_{60}/BCP/Al based OPVs are independent of the φ of the ITO electrode, by varying the ITO φ from 4.5 eV to 5.4 eV using fluorinated phosphonic acid nanolayers and air plasma treatment. In that case the φ of the ITO electrode did exceed the I_p of the donor ($I_p \sim 4.9$ eV)[28]. However, the full range of φ was achieved using very different surface treatments and the difference in φ between those that resulted in an ITO φ greater than the I_p of pentacene was very small; 0.1 eV ± 0.1 eV.[27] The latter also exhibited a very large difference in hydrophilicity, as evident from a ~100° difference in water contact angle. Since it is known that the growth mode of pentacene films is extremely sensitive to differences in substrate hydropilicity[28,29] the effect of the small change in φ cannot be differentiated from the affect of the large difference in electrode hydropilicity on the interfacial energetics. Other factors that complicate the interpretation of the data include: (i) the known instability of the φ change bought about by oxygen plasma treatment which renders these substrates unreliable for fundamental studies of interfacial energetics[30]; (ii) and the use of acidic nanolayers, since even very dilute acid solutions are known to etch ITO modifying the surface composition and liberating ions that can dope the organic semiconductor in the region close to the contact thereby drastically modifying its nature.[31–33]

Herein a solventless method for the chemical derivatization of ITO glass with a silane nanolayer is reported. To the authors' knowledge this is the first time this method of nanolayer deposition has been used for this purpose in the context of organic optoelectronics.[34,35] The advantage of vapor phase deposition in the current context is its amenability to scale-up, and thus integration into a commercial fabrication process. As a tool for studying the interfacial energetics this method has three distinct advantages over deposition from solution: (i) The absence of a solvent minimizes the likelihood of incorporating solvent molecules or impurities into the nanolayer.; (ii) Covalent coupling to the surface is afforded by methoxysilane moieties and so free protons are not produce upon chemisorption, thereby avoiding the complexity associated with the use of acidic anchor groups.; (iii) The byproduct of the condenzation reaction (methanol) is volatile and so does not remain at the interface when introduced into a vacuum system. We have used this approach to modify the surface potential of ITO glass using (3-chloropropyl)trimethoxysilane (CPS) and (3,3,3-trifluoropropyl)trimethoxysilane (FPS) (**Figure 1**(a)). These molecules were chosen because they modify the surface of ITO glass such that the difference in φ is large; ~ 0.5 eV, whilst being virtually identical in hydrophilicity, surface roughness, transparency and electrical conductivity. Furthermore, since they are of comparable size it can be assumed that the effective thickness of single layers of CPS and FPS is comparable (~0.8 nm).[35,36] Additionally, we show that the φ of ITO glass modified by silane nanolayers is very stable upon storage under nitrogen, in sharp contrast to that of UV/O_3 treated ITO glass which decreases rapidly from an initially high value. Collectively these properties make this pair of electrodes ideal for investigating the impact on OPV performance of positive space charge close to the
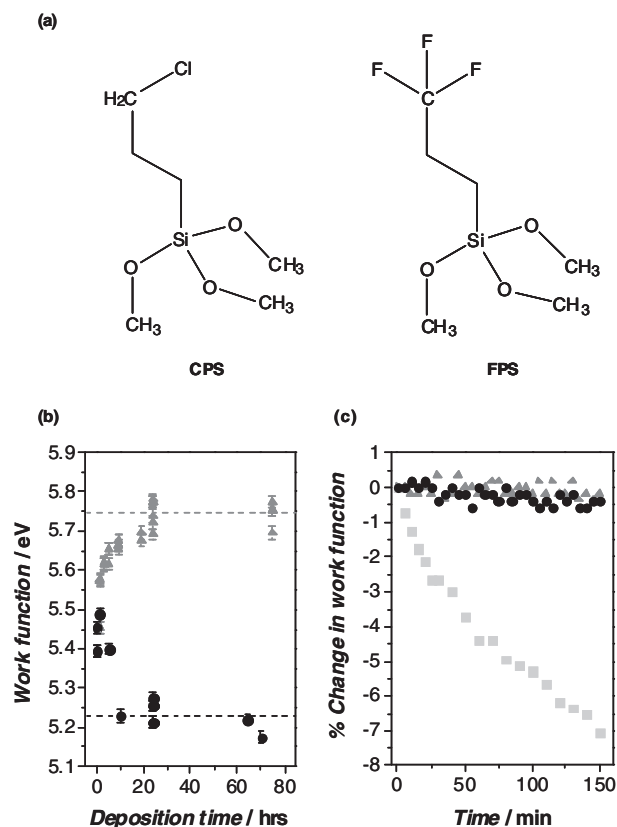
FULL PAPER

Figure 1. a) (3-chloropropyl)trimethoxysilane (CPS) and (3,3,3-trifluoropropyl)trimethoxysilane (FPS); b) Variation in the φ of ITO glass with exposure time to FPS (triangles) and CPS (circles) vapour at 5 mbar.; (c) Change in φ of ITO with time after treatment with FPS for 24 hours (triangles), CPS for 24 hours (circles) and UV/O$_3$ only (squares).

hole-extracting electrode. To ensure spontaneous electron-transfer from the organic semiconductor to both model electrodes a low I_p organic semiconductor was selected: namely pentacene, $I_p = 4.9$–5.0 eV.[28] Pentacene is also widely regarded as the prototypical conjugated organic molecule since it is the most intensively investigated organic semiconductor and its amenability to vacuum deposition allows a high degree of control over layer thickness and the environment in which the contact is formed.[16,37] In addition to varying the φ of the electrode, a picture of the extent and distribution of charge transferred across both interfaces upon contact formation is constructed by measuring the change in contact potential as a function of pentacene thickness, and correlated directly with the performance of bi-layer OPV devices employing C$_{60}$ as the electron acceptor. From the results of this judiciously designed study a generic electrode design rule is proposed with applicability to discrete heterojunction OPVs and those based on mixed heterojunctions sandwiched between single component donor and acceptor layers or continuously graded photoactive layers.[38,39] In addition, we show that the stability of the interface between pentacene and ITO is a critical determinant of device lifetime and present compelling evidence that silane nanolayers are a remarkably effective means of improving the stability of this interface.

2. Results and Discussion

2.1. Electrode Fabrication and Characterization

It is well known that molecules with methoxysilane moieties bind to oxide surfaces including ITO glass *via* strong siloxane linkages.[26,34–36] In order to optimize the deposition time the φ was measured as a function of the time freshly UV/O$_3$ treated substrates were exposed to FPS vapor at 5 mbar (Figure 1(b)). It is evident from Figure 1 that the change in φ saturates for t > 20 hrs, consistent with increasing coverage until the surface density is saturated.[23] The increase in φ to ~5.75 eV is consistent with FPS molecules oriented such that the electronegative –CF$_3$ moieties are at the nanolayer surface, since the inwardly pointing molecular dipole would operate to decrease the surface potential, thus increasing φ.[10,11,15,21–25] Ultra-low energy secondary ion mass spectroscopy (ule-SIMS) was used to provide direct evidence for FPS on the ITO surface. Mass spectra from the near-surface region were obtained using both O$_2^+$ and Cs$^+$ primary ions. Upon FPS deposition the measured secondary ion signal intensities for F$^-$, CF$_3^-$ and Si$^+$ were increased by a factor of 70, 200 and 10 respectively as compared to freshly UV/O$_3$ treated ITO glass. The signal intensity for the fragment ion most indicative of coupling to the ITO surface; SiOIn$^+$, was increased by 4-fold. The root-mean-square (rms) roughness of ITO glass derivatized with FPS measured using an Atomic Force Microscope (AFM) was identical to that of untreated ITO (~3.5 nm), evidence that polymerization of FPS does not occur to any significant extent using the vapor phase deposition method. This conclusion is in agreement with Aswal *et al.*[34] and Stec *et al.*[35] who used vapor phase deposition of trimethoxysilane nanolayers to immobilize incident Au atoms on silicon and glass substrates respectively, and is corroborated by the absence of ion fragments in the ule-SIMS spectra assigned to Si-O-Si linkages. Figure 1(b) also shows evolution of the φ of UV/O$_3$ treated ITO glass as a function of time exposed to CPS vapor, from which it is evident that the optimal exposure time is also >20 hrs and the φ of CPS derivatized ITO glass saturates at ~5.25 eV. Consequently for the purposes of this study the nanolayer derivatization time was fixed at 24 hours. Notably, it is clear from Figure 1(c) that, unlike freshly UV/O$_3$ treated ITO glass, the φ of CPS and FPS derivatizated ITO glass remains stable for extended periods in a nitrogen atmosphere, making them well suited as model high φ electrodes. The static water contact angle of ITO glass exposed to CPS and FPS for 24 hours was: 68° ± 3° and 73° ± 3° respectively. To verify that the growth mode of pentacene films at low thickness was not significantly impacted by this small difference in hydropilicity the complimentary techniques of electronic absorption spectroscopy and AFM imaging were used to probe for differences in the degree of crystallinity and size of crystallites in 5 nm and 45 nm films of pentacene deposited onto ITO glass derivatized with the CPS and FPS nanolayers (Figures 1S-4S). From the absence of any discernable differences in either the absorption spectrum or surface morphology it can be concluded that the pentacene growth mode on both substrate types is not significantly different.

www.MaterialsViews.com

www.advenergymat.de

ADVANCED
ENERGY
MATERIALS

FULL PAPER

This result is consistent with comprehensive studies of the growth and evolution of pentacene films on self-assembled monolayer terminated substrates by Hu et al.[40] and Käfer et al.[41], who have shown that pentacene molecules adopt a near vertical orientation with respect to the plane of the substrate regardless of the monolayer termination[40,41] even when the underlying substrate is polycrystalline.[41]

2.2. Measuring Interfacial Energetics

To probe the interfacial energetics upon contact formation the Kelvin probe (KP) technique was used to measure the change in energy of the vacuum level (ε_{vac}) relative to the ε^F, denoted as $\varepsilon_{vac}{}^F$, upon stepwise deposition of pentacene onto the CPS and FPS derivatized substrates. Measurements were made under nitrogen immediately after pentacene deposition without exposure to the laboratory atmosphere. Unlike UV photo-electron spectroscopy, which can also be used to make such measurements, the maximum film thickness that can be probed using the KP technique is not limited by sample charging.[15,20,42–44] As a result the change in potential across the full 45 nm pentacene film thickness used to fabricate OPV devices can be probed. In order to corroborate the conclusions pertaining to the establishment of electrical equilibrium upon contact formation measurements were also performed on freshly UV/O$_3$ treated ITO glass.

2.2.1. Fermi Level Alignment

Figures 2 shows how $\varepsilon_{vac}{}^F$ changes upon stepwise deposition of thin films of pentacene onto the three substrates ITO and FPS/ITO and CPS/ITO. In all cases $\varepsilon_{vac}{}^F$ rapidly decreases and saturates at a common value of ~4.6 eV consistent with the formation of an interfacial double layer resulting from the transfer of electron density from the pentacene overlayer into the ITO electrode. The convergence to a common value is compelling evidence that in all cases sufficient charge is transferred for thermodynamic equilibrium to be established, since an important criterion for ε^F alignment it that the measured φ of the organic over layer should be independent of the φ of the underlying substrate.[15,42,44] Seki et al.[15,42,44] point out that thermodynamic equilibrium across organic/electrode interfaces cannot be assumed for device thicknesses of undoped molecular semiconductors deposited under vacuum, since the density of unintentional impurities capable of donating/accepting charge is typically too low. At the interfaces studied herein the I_p of the molecular overlayer is less than the φ of the substrate and so the source of electron density is a high density of filled frontier molecular orbitals rather than a low density of unintentional impurities. Under these circumstances there is no bottleneck to achieving ε^F alignment across the interface for the film thicknesses used. Notably, the saturation value $\varepsilon_{vac}{}^F$ is ~0.3 eV lower in energy than expected for intrinsic pentacene, evidence of low levels of p-type impurities in the pentacene overlayer. Thin films of molecular semiconductors are known to be susceptible to low levels of unintentional doping, even when deposited under UHV conditions and so are to be expected under OPV fabrication conditions.[45]

2.2.2. Ground-State Charge Transfer

The insets in Figure 2 show the interfacial charge distribution $\rho(x)$ that would give rise to the profiles in Figure 2 as determined using Poisson's equation:

$$\frac{d^2 V(x)}{d x^2} = -\frac{\rho(x)}{\varepsilon_r \, \varepsilon} \qquad (1)$$

where ε is the permittivity of free space and ε_r is the relative permittivity of pentacene; 3.[46] It is evident that in all cases the positive space charge is located within a few nanometres of the interface, although the thickness coordinates can be regarded as upper limits since ultra-thin organic films rarely grow according to a layer-by-layer (Frank-van der Merwe) growth mode.[37]

Whilst the electronic structure and transport in molecular solids at room temperature is generally not described in terms of band theory, some highly crystalline high mobility solids
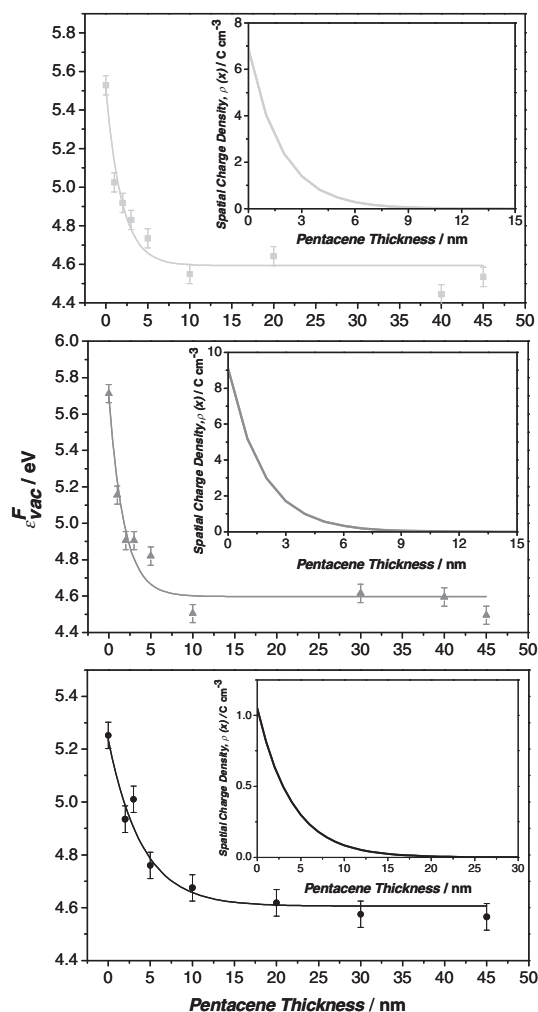

Figure 2. The variation in $\varepsilon_{vac}{}^F$ upon deposition of stepwise films of pentacene onto; i) freshly UV/O$_3$ treated ITO (upper); ii) FPS/ ITO glass (middle); iii) CPS/ ITO glass (lower). All φ measurements were made under N$_2$ immediately after pentacene deposition. The insets depict the space charge density distributions that would give rise to the variation in $\varepsilon_{vac}{}^F$.

ADVANCED
ENERGY
MATERIALS

www.advenergymat.de
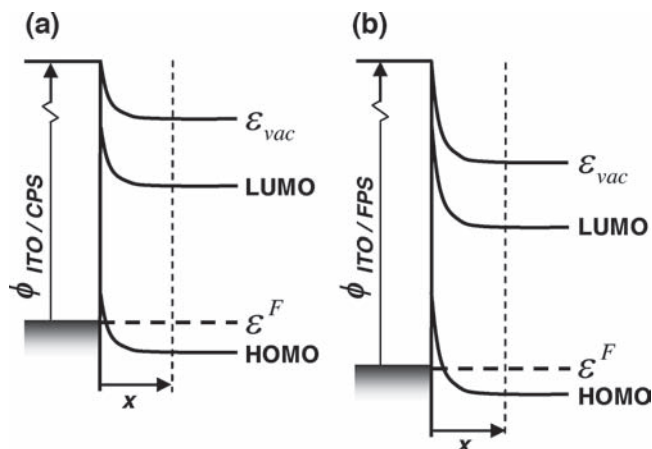
www.MaterialsViews.com

FULL PAPER

Figure 3. Schematic representation of the interfacial energetics at the interfaces: a) pentacene/CPS/ITO glass; and b) pentacene/FPS/ITO glass, assuming a band-type description of the electronic structure in the pentacene overlayer.

such as the acenes are an exception.[47] Evaporated pentacene films are invariably polycrystalline[28,29,37] and in this case the crystallite diameter is 50–100 nm, as determined using AFM (**S3 & S4**). At a local level the energetics at the pentacene/electrode interface can therefore be described in terms of abrupt bending of the pentacene bands across the space charge region as depicted in **Figure 3**. An alternative *molecular* model is one in which the Fermi level of the electrode is pinned to the positive polaron level of those pentacene molecules at the interface.[17] Regardless of its origin it is clear from Figure 2 that the positive space charge region in the pentacene layer is confined to the first few nanometres of the interface in all three cases[48] giving rise to large built-in electric field in the critical region close to the interface. By integrating under the curves of spatial charge density *vs.* distance (Figure 2 **(inset)**) the total space charge in the pentacene overlayer per unit area of interface can be quantified: The total space charge at the interface with FPS derivatized ITO ($\sim16.3 \times 10^{-7}$ C cm^{-2}) is four-fold larger than at the interface with CPS derivatized ITO ($\sim4.2 \times 10^{-7}$ C cm^{-2}).

2.3. Device Measurements

To investigate the impact on OPV performance of this large difference in space charge density in the critical region close to the interface with the hole-extracting electrode, model OPV devices were fabricated by sequential deposition of 40 nm C$_{60}$, 8 nm BCP and 1000 nm Al on top of the 45 nm pentacene layers. The performance characteristics for OPV devices incorporating ITO, ITO/CPS and ITO/FPS substrate electrodes under 1 sun simulated irradiance are summarized in **Table 1**. From Table 1 and the representative J/V characteristics shown in **Figure 4**, it is evident that none of the key device performance parameters are impacted by the large difference in the extent of the interfacial space charge region. Since the dark J/V characteristics (Figure 4 **(inset)**) are also virtually identical this is compelling

Table 1. Summary of the key device performance characteristics for OPVs with a device structure; ITO/X/pentacene/C$_{60}$/BCP/Al, where X is freshly UV/O$_3$ treated ITO glass (none) or a nanolayer of FPS or CPS.

	Nanolayer		
	None	CPS	FPS
J_{sc} [mA cm^2] ± 1 SD	7.0 ± 0.2	7.1 ± 0.2	7.3 ± 0.3
V_{oc} [Volts] ± 1 SD	0.40 ± 0.01	0.40 ± 0.01	0.41 ± 0.01
F.F. ± 1 SD	0.56 ± 0.02	0.57 ± 0.03	0.57 ± 0.3

evidence that the Schottky barrier to hole-injection, and thus the built-in electric field, are essentially identical, consistent with the establishment of ε^F alignment. The importance of this result lies in the demonstration that it is not necessary to engineer the φ of the hole-extracting electrode for OPVs beyond ensuring that it is greater than the I_p of the donor material, thus simplifying an important aspect of device design. This result rationalizes a recent report by our group that high φ gold nanoparticles ($\varphi \sim5.9$ eV) function as efficient hole-extraction materials in bilayer OPV devices based on donor materials with I_p's of ~5.3 eV and ~5.6 eV.[9] We propose that this electrode design rule will also be applicable to molecular OPVs employing mixed photoactive layers pinned between two single component layers. From Figure 4 it is clear that all devices exhibit a photocurrent of ~7 mA cm^{-2} under 1 sun simulated illumination. Assuming a built-in electric field of 1 V[49] and hole-mobility of ~1.0 cm^{-2} V^{-1} s^{-1} [28] this corresponds to a space charge density of $<10^{-6}$ C cm^{-3} in the interfacial region. Since the interfacial space charge density formed spontaneously upon contact formation (~1 C cm^{-3}) is many orders of magnitude larger than the photo-generated space charge density it can be concluded that the energy level diagrams derived from the KP measurements are good depictions of the interfacial energetics close to V_{oc} under operational conditions.
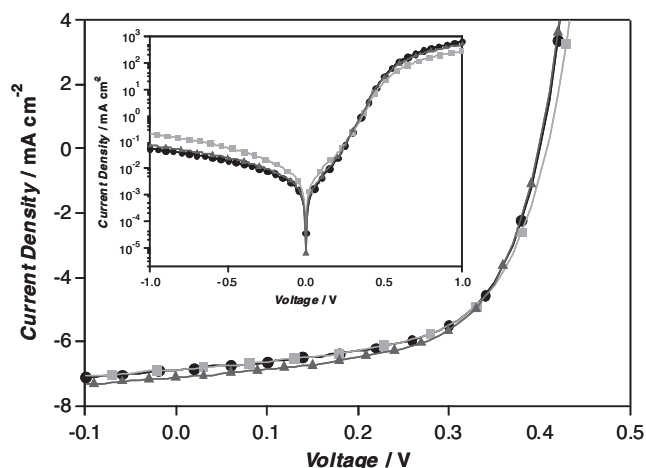

Figure 4. Representative $J–V$ characteristics for a ITO/X/pentacene/C$_{60}$/BCP/Al device under 1 sun simulated illumination, where X is freshly UV/O$_3$ treated ITO glass (squares) or a nano-layer of FPS (triangles) or CPS (circles). Inset: The corresponding dark JV characteristics.

2.4. Device Lifetime Studies

Beyond functioning as a tool to investigate the fundamentals of electrode design for OPVs vapour phase silanization is a scalable and potentially cost effective means of engineering the surface of ITO and other conducting oxide electrodes for this application. As the efficiency of OPVs edges towards the minimum required for commercialization the issue of operational lifetime has become increasingly important.[50–54] Whilst it is clear that the interfaces in OPVs are critical determinants of device lifetime, current understanding of the degradation mechanisms is at an early stage of development.[51,53] Having shown that the φ of ITO glass is stabilized by CPS and FPS nanolayers (Figure 1(c)), the possibility that this would translate to improvement device stability was explored. **Figure 5** summarizes typical key performance characteristics for OPVs with and without silane nanolayers over an extended period of continuous illumination. The J_{sc} of all devices is stable at ~7 mA cm^{-2}. The V_{oc} and FF of OPVs fabricated on freshly UV/O$_3$ treated ITO glass exhibit an initial rapid decline followed by gradual near-linear deterioration. Conversely the V_{oc} of OPVs incorporating silane nanolayers remains stable and the FF declines at a slow near-linear rate throughout. Since

the gradual deterioration in FF is common to OPVs with and without nanolayers it may not stem from deterioration of the ITO/pentacene interface, but from another degradation mechanism operating in parallel over the same time domain. The absence of the initial rapid decline in FF and any significant change in V_{oc} in OPVs incorporating silane nanolayers is compelling evidence that the stability of the ITO/pentacene interface is greatly improved. Since this improvement is also independent of the ITO electrode φ it is tentatively attributed to enhanced interfacial adhesion, since the polar hydroxyl and oxo moieties at the surface of ITO glass are known to render it poorly suited to the formation of robust interfaces with non-polar organic semiconductors.[55,56] A consequence of poor interfacial adhesion is an increased likelihood of delamination, which would manifest itself as an increase in device series resistance and deterioration in FF as observed in OPVs without a silane nanolayer. This result demonstrates the critical role that the pentacene/ ITO glass interface plays in determining the operational lifetime of these devices and offers a path to engineering this interface to extend device lifetime. To our knowledge the impact on OPV lifetime of using molecular nanolayers has not previously been reported and investigations are ongoing to verify the hypothesis that the observed improvement in device lifetime stems from an improvement in interfacial adhesion.

3. Conclusions

In summary, a solvent free protocol for the derivatization of ITO electrodes with a silane nanolayer is reported. Unlike deposition from solution, this method is scalable and a potentially cost-effective means of enhancing the functionality of ITO electrodes supported on glass or plastic substrates for application in organic optoelectronics. We show that dipolar silane nanolayers deposited from the vapor phase can be used to engineer large changes (~0.5 eV) in the work function and impart improved stability to this widely utilized transparent electrode material. Using this approach in conjunction with measurements of the interfacial energetics it is shown that the performance of model OPV devices based on pentacene/C$_{60}$ heterojunctions is independent of the extent of positive space charge density in the critical region close to the interface with the donor layer. This judiciously designed experiment demonstrates that it is unnecessary to engineer the φ of the hole-extracting electrode to match the ionization potential of the donor layer, rather only to ensure that former exceeds the latter, thus simplifying an important aspect of device design. In addition, we show that the stability of the interface between the ITO electrode and pentacene layer is a critical determinant of operational lifetime in pentacene/C$_{60}$ based OPVs and demonstrate the remarkable effectiveness of silane nanolayers in retarding device degradation. Notably, the results of this study could be applied directly to the manufacture of the current generation of flexible OPV, since high work function, stable ITO electrodes realized using silane nanolayers could be employed in place of the problematic hole-extracting material poly(3,4-ethylenedioxythiophene):poly(styrenesulfonate).
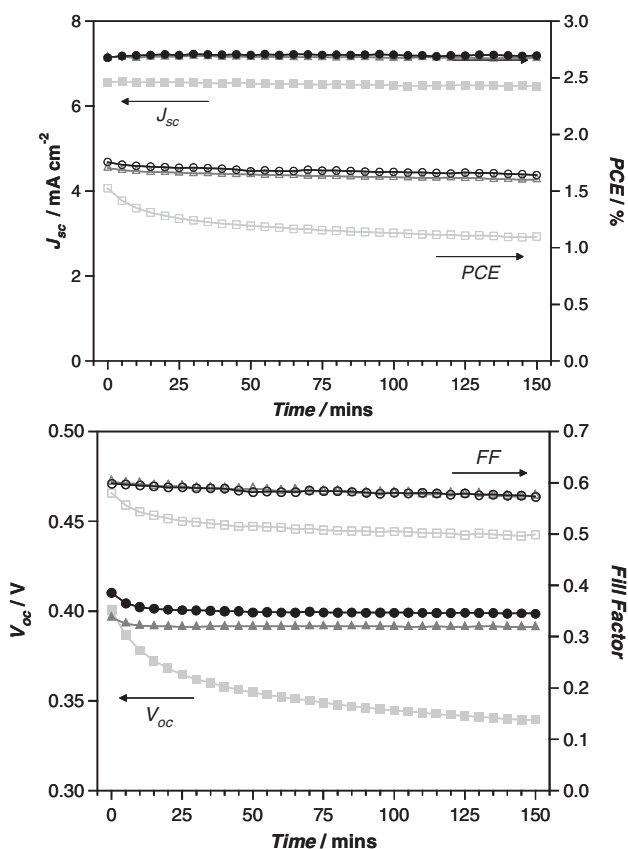

Figure 5. Variation of device performance parameters under 1 sun simulated solar irradiance as a function of time. The device structure is ITO/X/pentacene/C$_{60}$/BCP/Al where X is freshly UV/O$_3$ treated ITO glass (squares) or a nano-layer of FPS (triangles) or CPS (circles). All measurements were made in a nitrogen atmosphere.

FULL PAPER

4. Experimental Section

4.1. Work Measurements (Kelvin Probe)

All work function measurements were made in a nitrogen filled glove box using a Kelvin Probe referenced to freshly cleaved HOPG graphite.

4.2. Electrode Fabrication

ITO glass substrates were cleaned *via* ultra-sonication in: (i) acetone; (ii) Decon Neutracon: H_2O; (iii) H_2O; (iv) and finally propan-2-ol, before UV/O_3 (Novascan PSD-UVT) treatment immediately prior to transfer into the vacuum system. UV/O_3 treatment involved exposure of the relevant substrates to UV light from a Hg lamp (185 nm and 254 nm, 20 mW/cm^2) at a distance of 25 mm from the substrate in a sealed air filled chamber for 15 minutes followed by a 15 minute incubation period.

4.3. Ultra Low Energy Secondary Ion Mass Spectroscopy (uleSIMS)

Ultra-low energy secondary ion mass spectroscopy (uleSIMS) was performed using an Atomika 4500 quadrupole instrument to provide direct evidence for FPS on the ITO surface. Mass spectra from the near surface region were obtained using both O_2^+ and Cs^+ primary ions with energies of 250 eV and 500 eV respectively.

4.4. OPV Fabrication and Characterization

OPV cells were fabricated under high vacuum (~10^{-6} mBar) by thermal evaporation. The photoactive organic materials; pentacene (H. W. Sands triply sublimed) and C_{60} (Nano-C Inc., 99.5%) were purified once by thermal gradient sublimation prior to deposition. Pentacene, C_{60} and BCP were deposited at rates of 1 Ås^{-1}, 0.5 Ås^{-1} and 1 Ås^{-1} respectively. Al cathodes were deposited *in-situ* by evaporation through a shadow mask to give active device areas of 0.16 cm^{-2} (**S5**). Current-voltage (J–V) characteristics were measured using a Keithley 2400 SourceMeter and Solar Simulator. The light intensity was calibrated to AM1.5 (100 mW cm^{-2}) using a calibrated silicon diode with KG5 colour filter. More than 15 of each device type were fabricated. Lifetime measurements were performed in a nitrogen atmosphere (<1 ppm O_2; <1 ppm H_2O) at room temperature under continuous illumination (AM1.5 (100 mW cm^{-2})). Lifetime tests for each device type were repeated 3 times.

Supporting Information

Supporting Information is available from the Wiley Online Library or from the author.

[1] F. C. Krebs, T. D. Nielsen, J. Fyenbo, M. Wadstrøm, M. S. Pedersen, *Energy Environ. Sci.* **2010**, *3*, 512.
[2] F. C. Krebs, T. Tromholt, M. Jørgensen, *Nanoscale* **2010**, *2*, 873.
[3] F. C. Krebs, J. Fyenbo, M. Jørgensen, *J. Mater. Chem.* **2010**, *20*, 8994.
[4] B. Kippelen, J-L. Brédas, *Energy Environ. Sci.* **2010**, *2*, 251.
[5] M. Riede, T. Mueller, W. Tress, R. Schueppel, K. Leo, *Nanotechnology* **2008**, *19*, 424001.
[6] J. Alstrup, M. Jørgensen, A. J. Medford, F. C. Krebs, *ACS Appl. Mater. Interfaces* **2010**, *2*, 2819.
[7] R. Steim, F. R. Kogler, C. J. Brabec, *J. Mater. Chem.* **2010**, *20*, 2499.
[8] L-M. Chen, Z. Xu, Z. Hong, Y. Yang, *J. Mater. Chem.* **2010**, *20*, 2575.
[9] L-J. Pegg, S. Schumann, R. A. Hatton, *ACS Nano* **2010**, *4*, 5671.
[10] W. J. Potscavage, A. Sharma, B. Kippelen, *Acc. Chem. Res.* **2009**, *42*, 1758.
[11] S. Khodabakhsh, B. M. Sanderson, J. Nelson, T. S. Jones, *Adv. Funct. Mater.* **2006**, *16*, 95.
[12] N. R. Armstrong, P. A. Veneman, E. Ratcliff, D. Placencia, M. Brumbach, *Acc. Chem. Res.* **2009**, *42*, 1748.
[13] H. Aziz, Z. D. Popovic, *Chem. Mater.* **2004**, *16*, 4522.
[14] S. T. Lee, Z. Q. Gao, L. S. Hung, *Appl. Phys. Lett.* **1999** *75*, 1404.
[15] H. Ishii, K. Sugiyama, E. Ito, K. Seki, *Adv. Mater.* **1999**, *11*, 605.
[16] N. Koch, *J. Phys. Condens. Matter.* **2008**, *20*, 1.
[17] S. Braun, W. R. Salaneck, M. Fahlman, *Adv. Mater.* **2009**, *21*, 1450.
[18] J. Hwang, A. Wan, A. Kahn, *Mater. Sci. Eng. R* **2009**, *64*, 1.
[19] V. Chauhan, R. A. Hatton, P. Sullivan, T. S. Jones, S. W. Cho, L. Piper, A. deMasi, K. Smith, *J. Mater. Chem.*, **2010**, *20*, 1173.
[20] R. J. Davis, M. T. Lloyd, S. R. Ferreira, M. J. Bruzek, S. E. Watkins, L. Lindell, P. Sehati, M. Fahlman, J. E. Anthony, J. W. P. Hsu, *J. Mater. Chem.* **2011**, DOI:10.1039/C0JM02349C.
[21] S. A. Paniagua, P. J. Hotchkiss, S. C. Jones, S. R. Marder, A. Mudalige, F. S. Marrikar, J. E. Pemberton, N. R. Armstrong, *J. Phys. Chem. C* **2008**, *112*, 7809.
[22] S. F. J. Appleyard, M. R. Willis, *Opt. Mater.* **1998**, *9*, 120.
[23] S. J. F. Appleyard, S. R. Day, R. D. Pickford, M. R. Willis, *J. Mater. Chem.* **2001**, *10*, 169.
[24] F. Nüesch, L. Si-Ahmed, B. François, L. Zuppiroli, *Chem. Phys. Lett.* **1998**, *288*, 861.
[25] N. Peor, R. Sfez, S. Yitzchaik, *J. Am. Chem. Soc.* **2007**, *130*, 4158.
[26] J. S. Kim, J. H. Park, J. H. Lee, J. Jo, D-Y. Kim, K. Cho, *Appl. Phys. Lett.* **2007**, *91*, 112111.
[27] A. Sharma, A. Haldi, Jr. W. J. Potscavage, P. J. Hotchkiss, S. R. Marder, B. Kippelen, *J. Mater. Chem.* **2009**, *19*, 5298.
[28] M. Kitamura, Y. Arakawa, *J. Phys.:Condens. Matter.* **2008**, *20*, 184011 (and references therein).
[29] J. Park, J-H. Bae, W-H. Kim, S-D. Lee, J. S. Gwag, D. W. Kim, J. C. Noh, J. S. Choi, *Solid-State Electronics* **2010**, *54*, 1650.
[30] A. Sharma, B. Kippelen, P. J. Hotchkiss, S. R. Marder, *Appl. Phys. Lett.* **2008**, *93*, 163308.
[31] F. Nuesch, E. W. Forsythe, Q. T. Le, L. J. Rothberg, *J. Appl. Phys.* **2000**, *87*, 7973.
[32] N. R. Armstrong, C. Carter, C. Donley, A. Simmonds, P. Lee, M. Brumbach, B. Kippelen, B. Domercq, S. Y. Yoo, *Thin Solid Films* **2003**, *445*, 342.

[33] C. Carter, M. Brumbach, C. Donley, R. D. Hreha, S. R. Marder, B. Domercq, S. Yoo, B. Kippelen, N. R. Armstrong, *J. Phys. Chem. B* **2006**, *110*, 25191.

[34] D. K. Aswal, S. Lenfant, D. Guerin, J. V. Yakhmi, D. Vuillaume, *Small*, **2005**, *1*, 725.

[35] H. M. Stec, R. Williams, T. S. Jones, R. A. Hatton, *Adv. Func. Mater.* **2011**, DOI:10.1002/adfm.201002021.

[36] D. J. Dunaway, R. L. McCarley, *Langmuir*, **1994**, *10*, 3598.

[37] R. Ruiz, D. Choudhary, B. Nickel, T. Toccoli, K-C. Chang, A. C. Mayer, P. Clancy, J. M. Blakely, R. L. Headrick, S. Iannotta, G. G. Malliaras, *Chem. Mater.* **2004**, *16*, 4497.

[38] S. Uchida, J. G. Xue, B. P. Rand, S. R. Forrest, *Appl. Phys. Lett.* **2004**, *84*, 4218.

[39] L. Chen, Y. W. Tang, X. Fan, C. Zhang, Z. Z. Chu, D. Wang, D. C. Zou, *Org. Electron.* **2009**, *10*, 724.

[40] W. S. Hu, Y. T. Tao, Y. J. Hsu, D. H. Wei, Y. S. Wu, *Langmuir* **2005**, *21*, 2260.

[41] D. Käfer, L. Ruppel, G. Witte, *Phys. Rev. B* **2007**, *75*, 085309.

[42] H. Ishii, N. Hayashi, E. Ito, Y. Washizu, K. Sugi, Y. Kimura, M. Niwano, Y. Ouchi, K. Seki, *Phys. Stat. Sol. (a)* **2004**, *201*, 1075.

[43] S. R. Day, R. A. Hatton, M. A. Chesters, M. R. Willis, *Thin Solid Films*, **2002**, *410*, 159.

[44] H. Ishii, H. Oji, E. Ito, N. Hayashi, D. Yoshimura, K. Seki, *J. Luminescence* **2000**, *87–89*, 61.

[45] T. Nishi, K. Kanai, Y. Ouchi, M. R. Willis, K. Seki, *Chem. Phys. Lett.* **2005**, *414*, 479.

[46] O. D. Jurchescu, J. Baas, T. T. M. Palstra, *Appl. Phys. Lett.* **2004**, *84*, 3061.

[47] D. Ad. S. Filho, E.-G. Kim, J.-L. Bre´das, *Adv. Mater.* **2005**, *17*, 1072.

[48] Beyond 7 nm from the interface the space charge density in the pentacene overlayer is < 0.3 C cm^{-3}, which is close to the resolution of the technique.

[49] J. C. Nolasco, A. Sánchez-Díaz, R. Cabré, J. Ferré-Borrull, L. F. Marsal, E. Palomares, J. Pallarés, *Appl. Phys. Lett.* **2010**, *97*, 013305.

[50] N. Anscombe, T. Aernouts, *Nature Photon.* **2010**, *4*, 608.

[51] C. J. Brabec, S. Gowrisanker, J. J. M. Halls, D. Laird, S. Jia, S. P. Williams, *Adv. Mater.* **2010**, *22*, 3839.

[52] B. P. Rand, J. Genoe, P. Heremans, J. Poortmans, *Prog. Photovolt: Res. Appl.* **2007**, *15*, 659.

[53] M. Jørgensen, K. Norrman, F. C. Krebs, *Sol. Energy Mater. Sol. Cells* **2008**, *92*, 868.

[54] A. Moujoud, S. H. Oh, J. J. Hye, H. J. Kim, *Sol. Energy Mater. Sol. Cells* **2011**, *95*, 1037.

[55] N. R. Armstrong, C. Carter, C. Donley, A. Simmonds, P. Lee, M. Brumbach, B. Kippelen, B. Domercq, S. Y. Yoo, *Thin Solid Films* **2003**, *445*, 342.

[56] J. S. Kim, F. Cacialli, R. Friend, *Thin Solid Films* **2003**, *445*, 358.